DIAS-STP-86-49

FINAL REVISED SEPT 86

OPTICAL BISTABILITY IN SEMICONDUCTOR INJECTION LASERS

John G McInerney, PhD

Assistant Professor
Center for High Technology Materials
University of New Mexico
Albuquerque
NM 87131
USA

Daniel M Heffernan, PhD

Lecturer
School of Physical Sciences
National Institute for Higher Education
Glasnevin
Dublin 9
Ireland

and

Research Associate
School of Theoretical Physics
Dublin Institute for Advanced Studies
10 Burlington Road
Dublin 4
Ireland

ABSTRACT

This paper reviews optical bistability in semiconductor lasers, with particular reference to the potential switching speeds of the systems demonstrated to date. Devices which switch by redistributing a nearly constant number of carriers within the active region should be faster, though less stable, than systems whose transitions are attended by large changes in carrier numbers. One system of the former type, the self-focused coupled cavity laser, is analysed in some detail and is compared with the twin stripe laser and the Fabry-Perot laser amplifier.

1 INTRODUCTION

Optical bistability may be defined as the existence of two distinct, stable output states of an optical system for a single input state or range of states [1-6]. Bistability occurs as a result of a strong interaction between nonlinearity and feedback in a system, stability being conferred by saturation of the nonlinearity (uniform stability) and by losses (asymptotic stability). The result is a characteristic curve of the form illustrated in Figure 1. The phenomenon is of interest because it exemplifies a certain class of nonequilibrium phase transitions and because it has the potential to provide effective optical memory, switching, amplification, pulse shaping and binary logic.

Bistable systems demonstrated to date have employed nonlinearities in semiconductors, atomic vapours , liquid crystals and hybrid electro-optical systems. These nonlinearities have included intensity-dependent absorption and refraction in a resonant cavity, intensity-dependent refraction and plasmon excitation at an interface, self-focusing, temperature dependent absorption, refraction and output polarization.

The large resonant nonlinearities available near the bandgaps of semiconductors may be utilised to develop devices operating at low optical intensities and having short interaction lengths, particularly in guided-wave configurations. Such devices should have high speeds and require low powers, and hence may be fabricated with high density in integrated optical and optoelectronic circuits.

Bistable optical devices may be classified as intrinsic or hybrid : intrinsic devices feature optical feedback, usually by a resonant cavity, and require an optical or optoelectronic nonlinearity. Hybrid devices usually rely on electrical feedback and require an electro-optical nonlinearity. Further classification may be made according to the parameter(s) which distinguish between the upper and lower states. These parameters include power or intensity, polarization, centre frequency, temporal and spatial coherence. The most obviously useful systems are intrinsic, with bistable power characteristics, though other system types may be induced to behave in this way by the insertion of the appropriate spectral, spatial or polarizing filter(s).

It is convenient to distinguish further between active systems, which incorporate their own optical sources, and passive systems which do not. The input to a passive bistable device is always optical, while the input to an active device depends on how the source is to be excited : electronic input (usually injection current) is most common, though optical pumping and triggering is also possible. Passive devices include nonlinear Fabry-Perot etalons, nonlinear interfaces, self-focusing elements, liquid crystal light valves and electro-optic modulators with electrical feedback. Active devices include semiconductor laser oscillators and superluminescent Fabry-Perot amplifiers. The latter are classified as active devices because they feature internal gain even though they are driven by an external source. A thorough review of bistability in passive systems is contained in the monograph by Gibbs [1] and the review article by Abraham and Smith [2]. Active semiconductor devices are reviewed and compared with similar passive devices in the articles by Adams [7,8]. The expected advantages of active devices include speed, gain, sensitivity and the ability to drive other devices, but power dissipation and complexity may limit their use in parallel processing operations requiring high density.

This paper concentrates on active semiconductor devices, that is on bistable injection lasers and amplifiers. Following a brief survey of such systems, we offer a convenient classification based on the charge storage properties of the structure. We then compare devices which store carriers while in the lower state and which may therefore be expected to operate at high speeds and require low switching powers. This comparison focuses on the Fabry-Perot laser amplifier, the twin stripe laser and the self-focused coupled cavity laser. The latter device is analysed in some detail as part of this comparison.

2 BISTABILITY IN SEMICONDUCTOR LASERS

Semiconductor lasers exhibit bistability due to nonlinearities in absorption, gain, dispersion, waveguiding and selection of the output polarization. Pulse position bistability, in which gain-switched laser pulses take one of two stable positions within a clock cycle, has recently been reported [9], but this phenomenon does not conform to the usual definition of optical bistability as stated in Section 1, and will not be discussed in this paper.

2.1 BISTABILITY DUE TO NONLINEAR ABSORPTION OR GAIN

First proposed by Lasher [10] and subsequently demonstrated by Nathan et al. [11] and by Basov [12], absorptive bistability relies on the presence of saturable absorption : the system is essentially an integrated source and cavity containing a saturable absorber, and the absorber behaves as originally discussed by Szöke et al. [13], bleaching at switch-up to enable the feedback, and recovering at switch-down. The first approach was to divide one of the laser contacts into two or more segments and bias one segment below transparency (Figure 2a). The early work used GaAs homostructure lasers [10-12,14] while later experiments proposed by Paoli [15] using double heterostructure GaAs/GaAlAs [16-25] and GaInAsP [26-31] devices have demonstrated nanosecond switching times at milliwatt power levels. To observe bistability rather than unstable pulsations, it is necessary that the contacts to the gain and absorbing regions be well isolated. This is not easily accomplished : apart from parasitic conductance due to the presence of the highly-doped cap layer, there is an additional photoconductive component via the active region when the device is operating. With good inter-section isolation, absorptive bistability in twin-section lasers may be characterised by a single adjustable parameter [32], and is therefore readily controllable.

To overcome the problem of providing strong optical coupling while preserving electrical isolation, a second approach using two distinct devices strongly coupled in an external cavity was proposed [33]. This twin diode external cavity configuration (Figure 2b), in which one diode is biased to provide gain and the other saturable loss, has exhibited absorptive bistability [34,35]. An alternative scheme has been suggested by Suzuki et al. [36], who analyzed a standard double heterostructure laser with a $Ga_{0.95}Al_{0.05}As$ active layer and an i-GaAs absorbing layer deposited on one facet. Such a device has yet to be fabricated.

Contrary to expectations, the cleaved coupled cavity (C^3) laser (Figure 3) did not show absorptive bistability but rather bistability due to gain saturation with both cavities biased above threshold [37-39].

2.2 DISPERSIVE BISTABILITY

Bistability due to nonlinear refractive effects has been demonstrated using a laser diode in a dispersive external cavity [40-42] (Figure 4a), in C^3 lasers at milliwatt power levels using electrical triggering [43,44] (Figure 4b) and in Fabry-Perot laser amplifiers [45-50] (Figure 4c) using microwatt level optical triggering . In each case the system is tuned into and out of resonance by the changing optical length of the cavity. The C^3 laser switching times were a few nanoseconds, those of the amplifier slightly less than a nanosecond. Dispersive bistability in semiconductor lasers is due to an intensity dependent refractive index which arises not from a direct third-order nonlinearity of the form $n(I) = n_0 + n_2 I$ (n_0, n_2 are constants), but rather from the influence of injected carriers via a combination of a shift of the absorption edge, free-carrier plasma dispersion and temperature changes during operation.

2.3 POLARIZATION BISTABILITY

When a DH laser operates near its polarization transition temperature, slight changes of temperature induced by CW operation can result in significant changes in threshold gain for each polarization [51,52]. The concept of polarization transition temperature arises from the existence of stress in the laser structure due to cooling following high temperature lattice matched growth. This stress modifies the band structure and facet reflectivities [53] and is obviously temperature dependent : below the transition temperature most DH lasers are TM polarized, changing to TE at the transition point. Experiments by Chen and Liu have demonstrated bistability due to this effect in GaInAsP/InP lasers near 200 K, with switching speeds of the order of nanoseconds [54,55]. The difficulty with this method is that T_{pol} is a property of an individual device, depending on structure and treatment during fabrication. Furthermore, the temperature changes which are believed to drive the bistable transitions depend on thermal impedances. T_{pol} is usually ~ 200-250 K, though it may be possible to increase it to ~ 300 K by deliberate introduction of internal strain [51,52] with corresponding penalties in threshold current and reliability. Adams has suggested that the reduced threshold margin between TE and TM modes in distributed feedback lasers might be utilised for room temperature polarization bistability [7].

2.4 WAVEGUIDING BISTABILITY

Optical bistability due to nonlinear waveguiding has been analyzed [56] and demonstrated using closely coupled twin stripe lasers [57-60] (Figure 5a) and using the self-focused coupled cavity laser (SCCL) (Figure 5b), consisting of two wide stripe GaAs/GaAlAs diodes strongly coupled in an external ring resonator [61-64].

White et al. [57-60] have achieved switching between gain-guided modes crossing diagonally between stripes and a symmetrical mode confined by the real index guide formed by the dip in injected carrier concentration in the inter-stripe region. Sub-nanosecond switching in this system has been triggered electrically [57,58] and optically using milliwatt powers [59].

McInerney et al. [61-64] have achieved bistability in the SCCL, in which spatial hole burning in the cavity leads to nonlinear waveguiding and effective self-focusing [63]. The system is the active analogue of an arrangement proposed by Kaplan [65] and by Bjorkholm et al. [66] and demonstrated by Bjorkholm et al. [67] using a classical self-focusing element and an apertured retro-reflector. Both submicrosecond [64,68] and anomalously slow [62] switching have been observed in this system.

2.5 CLASSIFICATION OF BISTABLE SEMICONDUCTOR LASERS

Since bistability is synthesised from feedback and nonlinearity and stabilised by saturation and losses, the dynamical behaviour of a bistable system is governed by the characteristic times of each of these elements. The first and last of these times, the optical transit time and photon lifetime of the cavity, are determined by the length and quality factor of the cavity, and are largely independent of the precise details of the nonlinearity. Because most of the nonlinearities in semiconductor laser bistability respond, saturate and recover by moving charge carriers into, out of or within the active region, the remaining time constants depend critically upon the charge storage properties of the system. In waveguiding or modal bistability there is rearrangement of carrier distributions but little change in the total numbers of carriers present during bistable transitions. In absorptive bistability, on the contrary, the recombination rate in the upper state is far higher than that in the lower state, and consequently the overall carrier numbers must change drastically during bistable transitions.

Thus we make the distinction between 'storing' systems with carriers in place, undergoing rearrangement of the distributions but preserving roughly the same numbers of carriers in the active region, and 'non-storing' systems in which carrier dissipation is crucial to the nonlinearity, excited carriers being supplied or removed by optical absorption/recombination or movement along a resistive pathway during switching. [This distinction is analogous to that between reactive and resistive electronic devices according to their ability to store field energy during operation.] Most realistic systems undergo changes in carrier distributions and numbers, and so lie between these two extremes.

As a general rule, storing devices should be faster but less stable than non-storing devices. The latter are limited by carrier recombination times. Usually at least one of the states is below threshold, so the limiting response time is the spontaneous carrier lifetime, typically a few nanoseconds. All absorptive systems demonstrated to date have been limited in this way. Systems exhibiting purely waveguiding bistability should not be limited by carrier lifetimes and should be more sensitive to small changes in electrical or optical input than absorptive systems having comparable thresholds. They should also be less stable with respect to external perturbations. Dispersive systems, because they rely on carrier- and gain-induced index changes, usually involve changes in carrier numbers and distributions, and offer a useful compromise between speed, sensitivity and stability.

The most promising of the dispersive bistable devices demonstrated to date is the Fabry-Perot optical amplifier, by virtue of its sensitivity and relative simplicity. The remainder of this paper seeks to compare the switching performance of bistable semiconductor lasers, particularly the FP amplifier and the present examples of waveguiding bistability, the twin stripe laser and the self-focused coupled cavity laser. To facilitate this comparison, the next section contains an analysis of the latter system.

3 ANALYSIS OF THE SELF-FOCUSED COUPLED CAVITY LASER (SCCL)

In Sections 3.1 and 3.2 we present a summary of the procedure used to derive the quasi-static characteristics of the SCCL. More complete details are contained in Reference [63]. Following from the conclusions of this analysis, we proceed in Section 3.3 to estimate the critical power and limiting speed for bistable transitions of the system.

The self-focused coupled cavity laser is illustrated in Figure 6. Two anti-reflection coated 20 μm oxide stripe GaAs/GaAlAs DH diodes are coupled in a long external resonator consisting of four microscope objective lenses L1-L4 and high reflectivity plane mirrors M1-M4. The ring laser so formed is bi-directional. Bistability is achieved when one laser current is fixed within a certain range and the other varied slightly above the composite system threshold [61] (Figure 7). Towards the upper end of the range the loop collapses and slow, irregular pulsations are observed [62].

3.1 INDUCED WAVEGUIDING IN A SINGLE WIDE STRIPE LASER

Induced waveguiding in a single laser is analysed by solving the single-mode rate equations, the field equation and the boundary conditions (the relative permittivity distribution) self-consistently. We assume a fundamental Gaussian mode and use a paraxial approximation, to obtain the transverse distributions of the carrier density, refractive index and optical intensity. From these solutions a 'master equation' is derived which gives the light-current characteristics in inverse form. This result is then extended to the case of two coupled diodes in an external ring cavity and the resulting light-current characteristics compared with those observed experimentally.

The model is essentially that of Buus [69] with the addition of nonlinear waveguiding by spatial hole burning in the lateral (x) direction. The single-mode rate equations are written in the following form :

$$\frac{\partial N}{\partial t} = \frac{J}{ed} - \frac{N}{\tau_s} + D\frac{\partial^2 N}{\partial x^2} - \frac{c}{n_g} g\Gamma_x IS \qquad (1)$$

$$\frac{dS}{dt} = \frac{c}{n_g}\{G - \alpha_{act} - \frac{1}{L}\log\left[\frac{1}{R}\right]\}S + \beta\frac{N_{avg}}{\tau_s}, \qquad (2)$$

where $N(x,t)$ and $S(t)$ are the electron and photon densities in the active region of thickness d, J the injected current density, D the electron diffusion coefficient, n_g the group index, g the gain coefficient per unit length, Γ_x the confinement factor within the stripe in the lateral direction, τ_s the spontaneous carrier lifetime, α_{act} the internal (free-carrier and scattering) loss coefficient in the active region, L the laser length and R the power reflectance, β the spontaneous emission factor. $I(x,t)$ is the normalised lateral intensity distribution

$$I(x,t) = \frac{|E(x,t)|^2}{\frac{1}{W}\int_{\infty}^{\infty}|\bar{E}(x,t)|^2 dx}, \qquad (3)$$

while $N_{avg}(t)$ is the spatially averaged carrier density

$$N_{avg}(t) = \frac{1}{W}\int_{\infty}^{\infty} N(x,t)I(x,t)dx. \qquad (4)$$

The relative permittivity distribution is given by

$$\varepsilon(x,t) = n^2 - 2\Gamma_y n_{act} N(x,t)\Delta', \tag{5}$$

where n is the effective index of the active region, n_{act} the material index, Γ_y the vertical confinement factor and $\Delta' = -dn/dN$ assumed to be a positive constant. The net material gain factor G(t) for the lasing mode is

$$G(t) = \frac{1}{n}\left[\Gamma_y n_{act}\frac{1}{W}\int_{-\infty}^{\infty} g'(N) I(x,t)\,dx - (1-\Gamma_y) n_{pass}\alpha_{pass}\right], \tag{6}$$

with n_{pass} and α_{pass} the index and loss coefficient in the cladding layers and $g'(N) = g(N) - \alpha(N)$ the effective gain coefficient. Both g and α are assumed to be linear in N, with $g(N) = aN - b$ and $\alpha_{act} = a'N + b'$. Solving the rate equations (1) and (2) in the quasi-static limit, with negligible diffusion and consistently with the Helmholtz equation for the electric field $\dot{E}(x)$

$$\frac{d^2\dot{E}}{dx^2} + (k^2\varepsilon - \beta_z^2)\dot{E} = 0, \tag{7}$$

in which $k = 2\pi/\lambda_0$ is the free-space wavenumber and β_z the propagation constant, yields the carrier density distribution

$$N(x) = \frac{\frac{\tau_s J}{ed} + \frac{\tau_s cb}{n_g}\Gamma_x I(x)S}{1 + \frac{\tau_s ca}{n_g}\Gamma_x I(x)S} \quad . \tag{8}$$

Assuming a fundamental Gaussian mode

$$I(x) = \frac{1}{\sqrt{\pi}}\frac{W}{W_L}\exp(-x^2/W_L^2) \tag{9}$$

and restricting the analysis to $x << W_L$ gives an almost parabolic carrier density distribution whose width is intensity dependent and whose value at the centre is

$$N(0) = \frac{\frac{\tau_s J}{ed} + \frac{\tau_s cb}{n_g}\Gamma_x AS}{1 + \frac{\tau_s ca}{n_g}\Gamma_x AS} \quad , \tag{10}$$

where $A = (1/\sqrt{\pi})(W/W_L)$. The relative permittivity is similarly distributed and its value at the centre of the stripe is

$$n_0^2 = n^2 - 2\Gamma_y n_{act}\Delta' N(0) \tag{11}$$

which, upon substitution in the field equation (7), leads to an intensity dependent Gaussian beam waist $W_0 = W_L\sqrt{2} = (kn_0\sqrt{\Delta})^{-1}$, where $\Delta(I)$ is a function giving the intensity dependence of the relative permittivity distribution. Knowing the carrier density distribution we calculate the spatially averaged carrier density from (4) and substitute in the photon number rate equation (2), to arrive at the 'master equations' for induced waveguiding in the paraxial approximation

$$\frac{\tau_s J}{ed} - \frac{b}{a} = \frac{1}{k^2 n_{act}\Gamma_y \Delta' W_0^2} \frac{\left[1 + \frac{\tau_s ca}{n_g}\Gamma_x AS\right]^2}{\frac{\tau_s ca}{n_g}\Gamma_x AS} \qquad (12)$$

and

$$S\left[\Gamma_y (n_{act}/n)[(a-a')N_{avg} + (b-b')] - [1-\Gamma_y][n_{pass}\alpha_{pass}/n] - \alpha_{act} - \frac{1}{L}\log(\frac{1}{R})\right] + \beta n_g N_{avg}/\tau_s c = 0, \qquad (13)$$

which give the light-current characteristics : (13) gives W_0 as a function of J and S, and substitution in (12) gives J as a function of S.

3.2 INDUCED WAVEGUIDING AND BISTABILITY IN THE TWIN DIODE LASER

We extend the analysis to the case of two diodes coupled in an external cavity by writing two independent carrier density rate equations and a common rate equation for the photon density in the cavity. The resulting set of rate equations, neglecting diffusion and assuming a steady state, is

$$0 = \frac{J_i}{ed} - \frac{N_i}{\tau_s} - \frac{c}{n_g} g_i(N_i)\Gamma_{ix} I_i S \qquad (14)$$

and

$$0 = \frac{c}{n_g}\left[G_1 + G_2 - \alpha_{1act} - \alpha_{2act} - \frac{1}{L}\log\left[\frac{1}{R}\right]\right]S + \frac{\beta}{\tau_s}(N_{1avg} + N_{2avg}), \qquad (15)$$

where the subscript i takes the values 1 and 2 and the symbols have the same meanings as in Section 3.1. The expressions for the normalised intensities $I_i(x_i)$, average carrier densities N_{iavg}, relative permittivity distributions $\varepsilon_i(x_i)$, gain coefficients $g_i'(N_i)$ and mode gains G_i and the Helmholtz equations for the electric fields $\bar{E}_i(x_i)$ are exactly as before. Proceeding as in the previous section, we obtain instead of (12) the coupled equations

$$C\Theta^2 S^2 \left[\frac{\tau_s J_i}{ed} - \frac{b}{a}\right] = Y_i(1 + Y_i)^2 \qquad (16)$$

and

$$\frac{\left[\frac{\tau_s J_1}{ed} - \frac{b}{a}\right]}{1 + Y_1} + \frac{\left[\frac{\tau_s J_2}{ed} - \frac{b}{a}\right]}{1 + Y_2} + \frac{Y_1^2 + Y_2^2}{2C\Theta^2 S^2} = \mathcal{F}(S), \qquad (17)$$

where $\Theta = \tau_s ca/n_g$ and $C = 2k^2 n_{act} \Delta' W^2/\pi$ are constants, $Y_i = \surd(\pi/2)(W/W_{i0})\Theta S$ the photon number normalised in each diode, and $\mathcal{F}(S)$ an intensity dependent function given by

$$\mathcal{F}(S) = \frac{\alpha_{tot} S}{\frac{n_{act}}{n}(a - a')S + \beta\frac{n_g}{\tau_s c}} - \frac{2b}{a}, \qquad (18)$$

where α_{tot} is the total loss coefficient for both diodes :

$$\alpha_{tot} = \alpha_{1act} + \alpha_{2act} + \frac{2n_{act}}{n}(b - b') + \frac{1}{L}\log\left[\frac{1}{R}\right]. \qquad (19)$$

Equations (16) and (17) are used to calculate the light-current characteristic curves of the SCCL. To compare with experimental results we fix one current (say J_2) and obtain the single remaining light-current characteristic. For fixed J_2 we find Y_2 (using (16) with i=2) as a function of S, substituting in (17) and using (16) with i=1 gives the desired relationship

$$\frac{\tau_s J_1}{ed} = \frac{b}{a} + \frac{1}{27C\theta^2 S^2}\left[\sqrt{(1 + 6\mathcal{G}(S))} - 1\right]\left[\sqrt{(1 + 6\mathcal{G}(S)} + 2\right]^2, \tag{20}$$

where

$$\mathcal{G}(S) = C\theta^2 S^2 \mathcal{F}(S) - \frac{(3Y_2^2 + 2Y_2)}{2} . \tag{21}$$

Obtaining the real light-current characteristic from the S-J_1 relation above is a trivial calculation, leading to the results shown in Figures 8 and 9. The values used in the calculations are given in Table 1, and the results are in good agreement with experiment. Because we have limited our analysis to the lowest mode in the paraxial approximation, we are unable to predict the saturation and eventual collapse of the bistability by such processes as gain-induced anti-guiding, filamentation, mode conversion or thermal effects.

3.3 ESTIMATION OF CRITICAL POWER FOR SELF-FOCUSING

Here we treat the induced waveguiding in the system in a manner analogous to the analysis of bistability by self-focusing as developed by Bjorkholm et al. [67]. The system, which is the passive analogue of the SCCL, is illustrated schematically in Figure 10. The refractive index of the self-focusing medium depends on intracavity intensity as $n(I) = n_0 + n_2 I$. The Gaussian beam propagates according to the equation

$$w(z) = w(0)\sqrt{[1 + (1 - P_{in}/P_{cr})(2z/B)^2]}, \qquad (22)$$

where $w(z)$ is the beam waist, P_{in} the input power and B the confocal parameter $(2\pi n_0/\lambda_0)w(0)^2$ of the beam. The critical power for self-focusing is given by

$$P_{cr} = (\lambda^2/4\pi^2)(1/8n_2) \qquad (23)$$

provided that the length ℓ of the self-focusing element is sufficient that $4\ell^2/B^2 >> 1$. The confocal parameter in our system is approximately 20 μm and the length of each element is 500 μm, so that this condition is easily satisfied. We use a simplified analysis of spatial hole burning to derive an equivalent n_2 for our system and hence obtain a critical intracavity power using (23). The result should give an order-of-magnitude estimate of the critical intracavity power for switching in the SCCL.

The situation is illustrated in Figure 11. The injected current density profile J(x) is depleted near the centre of the stripe by a (subtractive) recombination current $J_R(x)$ due to hole burning. This is given approximately by

$$J_R(x) = g(x)I(x)ed/h\nu, \tag{24}$$

where g and I are the lateral distributions of gain and intensity and ν the laser frequency. Since the system is near threshold, the depression in carrier density near the centre due to the hole burning may be written as

$$\Delta N(x) \approx -J_R(x)\tau_s/ed, \tag{25}$$

with a corresponding local increase in refractive index

$$\Delta n(x) \approx \Delta N(x)(dn/dN) = -\Delta' \Delta N(x)$$

$$\approx \Delta' g(x)I(x)\tau_s/h\nu. \tag{26}$$

Hence an equivalent n_2 (from $\Delta n = n_2 I$) for our system is

$$n_2 \approx \Delta' g \tau_s / h\nu, \tag{27}$$

from which we estimate the critical power to be

$$P_{cr} \approx hc\lambda_0 / 32\pi^2 \Delta' g \tau_s. \tag{28}$$

Using the values given in Table 1 and $g \approx \xi(J_{nom} - J_0)$ with $\xi = 40$ $cm^{-1}(kA\ cm^{-2}\ \mu m^{-1})^{-1}$ and $J_0 = 5.0$ kA cm^{-2} μm^{-1} we find $g \approx 100$ cm^{-1} under the conditions of the experiment, and calculate $P_{cr} \approx 4$ mW, in reasonable agreement with the intracavity powers measured in the SCCL at the switching transitions. This result is also consistent with the results of a more thorough analysis by Kirkby et al. [70], who estimate that self-focusing becomes significant at 6 mW in DH 20 μm oxide stripe GaAs/GaAlAs lasers. Sommers [71] calculates a critical power for lateral hole burning in oxide stripe lasers based on an original model by Hakki [72], and obtains figures in the region of 10-20 mW based on a more drastic definition of critical power.

4 COMPARISON OF DYNAMICAL BEHAVIOUR OF BISTABLE SEMICONDUCTOR LASERS

A detailed discussion of the dynamical behaviour of bistable lasers would require numerical analysis based on the semi-classical (coupled Maxwell-Bloch) equations with feedback-controlled boundary conditions [1,5,6]. A qualitative understanding of such details as overdriven switching times, critical slowing down, regenerative pulsations and bifurcation from a stable state through a hierarchy of instabilities can be gained by analogy with other systems undergoing a non-equilibrium first-order phase transition and hence governed by similar equations. Even if we were to neglect all phase relations in the semi-classical equations, thereby confining ourselves to a discussion of quasi-equilibrium switching times and damped relaxation oscillations using a rate equation approach, any such discussion would require the inclusion of diffusion and delayed feedback terms in the rate equations. This problem is far beyond the scope of the simple analysis presented in Section 3. Accordingly, we restrict ourselves here to some general and qualitative remarks on the potential switching times of bistable laser devices, particularly in compound cavity absorptive systems, the self-focused coupled cavity, the twin stripe laser and the superluminescent Fabry-Perot amplifier.

In considering the dynamical behaviour of a bistable device it is essential to include the recovery time, which will limit the cycling rate in repetitive operations (for example, in logic systems).

It has already been pointed out in Section 2.5 that there are four characteristic times which determine the dynamical behaviour of a bistable system. These are :

(1) the optical transit time;

(2) the cavity photon lifetime;

(3) the nonlinearity response time;

(4) the time constant of the saturation process.

The switch-up time will be determined by (1), (3) and (4), the switch-up threshold being determined by the cavity loss rate and hence by (2). The switch-down time will be determined initially by (1), (2) and (3), with an eventual recovery time determined by the relaxation rate of the excited state. Recovery requires that the lower state photon and carrier numbers be reset, which requires several photon and carrier lifetimes.

The round trip time depends only on the cavity optical length, the photon lifetime on the quality factor of the cavity. The response time of the nonlinearity is determined by the time constants of generation and recombination as well as any other mechanisms involved. It is usually negligible in carrier storing systems unless thermal effects are involved. In the latter case the response time is at best hundreds of picoseconds and usually longer : the time constant is

$$\tau_{th} \sim d^2/8D_{th} \qquad (29)$$

for a bi-directional thermal diffusion process from a region of characteristic dimension d (in this case the active layer thickness) in a medium of thermal diffusivity D_{th} (≈ 0.3 cm^2 s^{-1} for GaAs, values for GaAlAs, InP and GaInAsP not available). The saturation time constant in semiconductor laser systems is usually limited by carrier diffusion, effects such as gain antiguiding set up to saturate self-focusing due to spatial hole burning being extremely rapid. In small, low-Q devices the carrier diffusion times between states will ultimately limit the switching speeds.

4.1 SWITCHING TIMES

The following discussion applies to systems where switching is due to a nonlinear refractive index, as where the cavity is swept into resonance by its changing optical length, or where the modal characteristics switch due to a changing index distribution. It is formulated specifically for a nonlinear Fabry-Perot or ring cavity containing a Kerr-like medium (intensity-dependent index $n(I) = n_0 + n_2 I$), for which the time dependence of the output field is

$$\tau_c \frac{\partial \tilde{E}_T}{\partial t} + \left[1 - R \exp\{j\Delta\phi(t)\}\right]\tilde{E}_T(t) = \tilde{E}_0(t + \tau_c), \qquad (30)$$

where $\tilde{E}_0(t)\exp(-j\omega t)$ is the field in the cavity at the output coupler, $\tilde{E}_T(t)\exp(-j\omega t)$ the field transmitted by the same output coupler, τ_c is the cavity round trip time and $\Delta\phi(t)$ the round trip phase change. The field equation is coupled by $\Delta\phi(t)$ to an equation expressing the time-dependence of the spatially-averaged refractive index, e.g. a Debye equation

$$\tau_R\left[1 + \frac{\partial}{\partial t}\right]\Delta\phi(t) = \delta + \kappa|E_T|^2 \qquad (31)$$

in which δ is the initial phase detuning, τ_R the convolved impulse response and saturation times (effective Debye relaxation time) of the nonlinearity, κ is a nonlinear coefficient which depends on the photon lifetime and is also proportional to the effective Kerr constant n_2. These equations give the time evolution of the output field and round trip phase change for slowly-varying input conditions : they are equivalent to adopting a slowly-varying envelope approximation [73], and give a lower limit for the switching response : clearly the switching time is limited by τ_c and τ_R. They also predict such phenomena as overshoot and damped oscillation (ringing) [74,75]. Finally, the switching times are affected not only by the rise time of the excitation but also by its amplitude : critical slowing down occurs when the amplitude of the switching stimulus approaches its threshold value [1,5,6].

4.2 RECOVERY TIMES

Recovery of a bistable laser requires not only switch-off but also relaxation of the excited state : the carrier and photon numbers in the lower state must be reset, and this takes a few carrier and photon lifetimes. Systems which store carriers in the lower state are expected to recover more rapidly than those which do not, and if the lower state is below threshold recovery will be limited by the spontaneous rather than the stimulated lifetime. Recovery times for absorptive systems are therefore expected to be several nanoseconds, those for subthreshold dispersive systems a few nanoseconds. These estimates are consistent with the results of experiments by Westlake et al. [50], who have measured limiting cycling rates for bistable Fabry-Perot amplifiers to be ≈ 250 MHz. The limitation of the recovery time of a passive system by its carrier lifetime has been demonstrated by altering this lifetime in an etched GaAs etalon [76] and in a proton-bombarded GaAs/GaAlAs multiple quantum-well excitonic absorber [77]. The recovery times of small, low-Q, carrier storing devices should be limited only by the switch-down times.

4.3 LIMITATIONS ON DYNAMICAL BEHAVIOUR

Twin-section or twin-diode absorptive systems are limited by switching delays and long relaxation times due to spontaneous recombination of excited electrons in the absorber. Though the high carrier densities present at saturation may lead to initial lifetime shortening, a rate equation analysis of twin diode lasers has shown switching delays and transition times limited to a few nanoseconds by the spontaneous carrier lifetime [33]. The scheme proposed by Suzuki et al. [36] using a saturably absorbing layer deposited on one facet may have shorter switching delay and rise time, but is still limited by a recovery time of some nanoseconds.

The self-focused coupled cavity laser, which used a long, high-Q resonator, is presently limited by its optical transit time and photon lifetime to switching times slightly less than a microsecond. The present implementation using macroscopic optics, whose physical size requires a long cavity, could be replaced by a smaller integrated version with a shorter photon lifetime, lower Q and the elimination of alignment difficulties and consequent lack of long-term stability. The ultimate limitation is the carrier diffusion time between the self-focused Gaussian profiles corresponding to the upper and lower states given by equation (8). If the width changes by ΔW_0 from an initial width W_0 in a bi-directional process in which the diffusion fronts are themselves Gaussian-like, the process is very fast, having a time constant

$$\tau_D \approx W_0 \Delta W_0 / 2D, \qquad (32)$$

where D ($\approx$ 78 cm^2 s^{-1} for lightly p-doped GaAs) is the electron diffusion coefficient. Using the expression $W_0 = \{kn_0\sqrt{\Delta(I)}\}^{-1}$, knowing the function $\Delta(I)$ (see [63]) and the photon numbers in the upper and lower states, we calculate a reasonable limit for τ_D to be a few tens of picoseconds. Considering the transit time and loss rate in an integrated device of physically realistic construction, this would indicate a limit to the switching time of a SCCL of slightly less than 100 ps.

In the case of the twin stripe laser, which is already an integrated device and is not limited by size or loss rate, the limit should again be the carrier diffusion time between states. Here the diffusion process is a unidirectional one across a distance ℓ (about half of the inter-stripe distance) and should have a time constant

$$\tau_{TS} \approx \ell^2/D \qquad (33)$$

which is of the order of 200 ps for stripes separated by 3 μm. This is greater than the postulated limit for the SCCL, but the twin stripe laser has the advantages of simpler construction and greater ease of optical triggering. The above estimate is consistent with the analysis by Shore and Rozzi [78] of transverse switching in single stripe lasers, predicting oscillation frequencies of the order of 10 GHz.

In the superluminescent Fabry-Perot amplifier, carrier diffusion should be extremely rapid, but the device is believed to be limited to slightly sub-nanosecond switching times and nanosecond recovery times by the spontaneous carrier lifetime [8,49,50]. It is, however, a useful compromise between the two extremes of absorptive and waveguiding bistability, having optical gain, reasonable stability, moderate speed and excellent sensitivity to optical input signals. Its simple structure should make parallel construction possible, although limitation in output power (due to the saturation intensity of $\sim 10^5$ W cm^{-2}) and power dissipation many times that of comparable passive devices (e.g. GaAs/GaAlAs multiple quantum well dispersive etalons) may limit the utility of this approach. Finally, it may be possible to achieve faster spectral bistability in the FP amplifier by tuning the frequency rather than the intensity of the input signal.

5 CONCLUSIONS

We have surveyed the achievement of optical bistability in semiconductor lasers. Systems which switch by redistributing a nearly constant number of carriers should be faster, though less stable than systems which switch with large changes of carrier numbers. One system of the former type, the self-focused coupled cavity laser, is analysed in some detail and is compared with the twin stripe laser and the Fabry-Perot optical amplifier. It is estimated that the potential switching speeds of the self-focused twin diode laser and the twin stripe laser are of the order of a hundred picoseconds, that of the amplifier several hundred picoseconds. The amplifier enjoys a significant advantage (as much as three orders of magnitude) in sensitivity and possesses optical gain , but is limited in cycling rate by spontaneous carrier relaxation and in output power by saturation effects.

6 ACKNOWLEDGEMENTS

Some of this work was carried out while one of us (JGM) was with the Microelectronics Research Group, Cavendish Laboratory, University of Cambridge, on a Research Fellowship sponsored by Standard Telecommunication Laboratories Ltd., whom we thank for this support. We also acknowledge financial assistance from Robinson College, Cambridge and the Irish National Board for Science and Technology. We are grateful to the referees and to Prof. M. Osiński, University of New Mexico, for valuable comments on the manuscript.

7 REFERENCES

1 Gibbs, H. M. : "Optical bistability : controlling light with light", Academic Press, Orlando, FL, 1985.

2 Abraham, E. and Smith, S. D. : "Optical bistability and related devices", Rep. Prog. Phys., 1982, 45, pp. 815-885.

3 Bowden, C. M., Ciftan, M. and Robl, H. R. (eds.) : "Optical bistability", Plenum Press, New York, 1981.

4 Bowden, C. M., Gibbs, H. M. and McCall, S. L. (eds.) : "Optical bistability 2", Plenum Press, New York, 1984.

5 Lugiato, L. A. : "Optical bistability", Contemp. Phys., 1983, 24, p. 333.

6 Lugiato, L. A. : "Theory of optical bistability", in Progr. in Opt., Vol. XXI (E. Wolf, ed.), North-Holland, Amsterdam, 1984, p. 69 et seq.

7 Adams, M. J. : "A tentative assessment of semiconductor laser optical bistability", Int. J. Electron., 1986, 60, pp. 123-142.

8 Adams, M. J., Westlake, H. J., O'Mahony, M. J. and Henning, I. D. : "A comparison of active and passive optical bistability in semiconductors", IEEE J. Quantum Electron., 1985, QE-21, pp. 1498-1504.

9 Gallagher, D. F. G., White, I. H. and Carroll, J. E. : "Pulse position bistability in injection lasers", CLEO '86, San Francisco, paper FH4.

10 Lasher, G. J. : "Analysis of a proposed bistable injection laser", Solid-State Electron., 1964, 7, pp. 707-716.

11 Nathan, M. I., Marinace, J. C., Rutz, R. F., Michel, A. E. and Lasher, G. J. : "A GaAs injection laser with novel mode control and switching properties", J. Appl. Phys., 1965, 36, pp. 473-480.

12 Basov, N. G. : "Dynamics of injection lasers", IEEE J. Quantum Electron., 1968, QE-4, pp.855-864.

13 Szöke, A., Daneu, V., Goldhar, J. and Kurnit, N. A. : "Bistable optical element and its applications", Appl. Phys. Lett., 1969, 15, pp. 376-379.

14 Lee, T. P. and Roldan, R. H. R. : "Repetitively Q-switching light pulses from GaAs injection lasers with tandem double-section stripe geometry", IEEE J. Quantum Electron., 1970,

QE-6, pp. 339-352.

15 Paoli, T. L. : "Saturable absorption effects in the self-pulsing (AlGa)As laser", Appl. Phys. Lett., 1979, 34, pp. 652-655.

16 Carney, J. K. and Fonstad, C. G. : "Double-heterojunction laser diodes with multiply segmented contacts", Appl. Phys. Lett., 1981, 38, pp. 303-305.

17 Goldobin, I. S., Kurnosov, V. D., Luk'yanov, V. N., Pak, G. T., Semenov, A. T., Shelkov, N. V., Yakubovich, S. D., and Yashumov, I. V. : "Bistable cw injection heterolaser", Sov. J. Quantum Electron., 1981, 11, pp. 526-527.

18 Harder, C., Lau, K. Y., and Yariv, A. : "Bistability and pulsations in CW semiconductor lasers with a controlled amount of saturable absorption", Appl. Phys. Lett., 1981, 39, pp. 382-384.

19 Harder, C., Lau, K. Y. and Yariv, A. : "Bistability and pulsations in semiconductor lasers with inhomogeneous current injection", IEEE J. Quantum Electron., 1982, QE-18, pp. 1351-1360.

20 Harder, C., Lau, K. Y. and Yariv, A. : "Bistability and negative resistance in semiconductor lasers", Appl. Phys. Lett., 1982, 40, pp. 124-126.

21 Lau, K. Y., Harder, C. and Yariv, A. : "Dynamic switching characteristics of a bistable injection laser", Appl. Phys. Lett., 1982, 40, pp. 198-200.

22 Lau, K. Y., Harder, C. and Yariv, A. : "Interaction of a bistable injection laser with an external optical cavity", Appl. Phys. Lett., 1982, 40, pp. 369-371.

23 Carney, J. K. and Fonstad, C. G. : "Effect of longitudinal variations in current injection and carrier concentration in laser diodes", IEEE J. Quantum Electron., 1983, QE-19, pp. 22-28.

24 Borodulin, V. I., Konyaev, V. P., Novikova, E. R., Tager, A. A., Tregub, D. P. and Elenkrig, B. B. : "Experimental investigation of inhomogeneously pumped injection lasers", Sov. J. Quantum Electron., 1983, 13, pp. 398-401.

25 Goldobin, I. S., Luk'yanov, V. N., Semenov, A. T., Solodkov, A. F., Tabunov, V. P. and Yakubovich, S. D. : "Two-component spatially inhomogeneous (GaAl)As heterojunction laser", Sov. J. Quantum Electron., 1983, 13, pp. 864-867.

26 Kawaguchi, H. and Iwane, G. : "Bistable operation in semiconductor lasers with inhomogeneous injection", Electron. Lett., 1981, 17, pp. 167-168.

27 Kawaguchi, H. : "Bistable operation of semiconductor lasers by optical injection", Electron. Lett., 1981, 17, pp.741-742.

28 Kawaguchi, H. : "Optical input and output characteristics for bistable lasers", Appl. Phys. Lett., 1982, 41, pp. 702-704.

29 Kawaguchi, H. : "Optical bistable-switching operation in semiconductor lasers with inhomogeneous excitation", IEE Proc. Pt. I (SSED), 1982, 129, pp. 141-148.

30 Kawaguchi, H. : "Bistability and differential gain in semiconductor lasers", Jpn. J. Appl. Phys., 1982, 21, Suppl. 21-1, pp. 371-376.

31 Odagiri, Y., Komatsu, K. and Suzuki, S : "Bistable laser-diode memory for optical time-division switching applications", Int. Conf. on Lasers and Electro-Opt. (CLEO '84), Anaheim, CA, June 1984, paper ThJ3.

32 Heffernan, D. M. : "Single-parameter characterization of bistability in double contact injection lasers", Phys. Lett., 1983, 94A, pp. 106-108.

33 Dziura, T. G. and Hall, D. G. : "Bistable operation of two semiconductor lasers in an external cavity : rate-equation analysis", IEEE J. Quantum Electron., 1983, QE-19, pp. 441-8.

34 Stallard, W. A. and Bradley, D. J. : "Bistability and slow oscillation in an external cavity semiconductor laser", Appl. Phys. Lett., 1983, 42, pp. 858-859.

35 McInerney, J. G. P. : "Semiconductor laser studies", Ph.D. dissertation, University of Dublin, Trinity College, 1984 (unpublished); the existence of saturable absorption in this laser was exploited to produce bandwidth-limited picosecond pulses by hybrid active-passive mode-locking, as reported by McInerney, J., Reekie, L. and Bradley, D. J. : "Generation of bandwidth-limited picosecond pulses by hybrid mode-locking an external cavity ring laser", Electron. Lett., 1985, 21, pp. 117-118.

36 Suzuki, Y., Shimada, J. and Yamashita, H. : "High-speed optical-optical logic gate for optical computers", Electron. Lett., 1985, 21, pp. 161-162.

37 Dutta, N. K., Agrawal, G. P. and Focht, M. W. : "Bistability in coupled cavity semiconductor lasers", Appl. Phys. Lett., 1984, 44, pp. 30-32.

38 Agrawal, G. P. and Dutta, N. K. : "Optical bistability in coupled-cavity semiconductor lasers", J. Appl. Phys., 1984, 56, pp. 664-669.

39 Phelan, P., Reekie, L., Bradley, D. J. and Stallard, W. A. : "Hysteretical and spectral behaviour of bistable cleaved coupled cavity semiconductor diode lasers", Opt. Quantum Electron., 1986, 18, pp. 35-41.

40 Bazhenov, V. Y., Bogatov, A. P., Eliseev, P. G., Okhotnikov, O. G., Pak, G. T., Rakhvalsky, M. P., Soskin, M. S., Taranenko, V. B. and Khairetdinov, K. A. : "Bistable operation and spectral tuning of an injection laser with an external dispersive cavity", IEE Proc. Pt. I (SSED), 1982, 129, pp. 77-82.

41 Glas, P. and Müller, R.: "Bistable operation of a GaAs-AlGaAs diode laser coupled to an external resonator of narrow spectral bandwidth", Opt. Quantum Electron., 1982, 14, pp. 375-389.

42 Glas, P., Klehr, A. and Müller, R.: "Transient and stationary properties in bistable operation of a GaAs laser coupled to an external resonator", Opt. Commun., 1983, 44, pp. 196-200.

43 Olsson, N. A., Tsang, W. T., Logan, R. A., Kaminow, I. P. and Ko, J.-S. : "Spectral bistability in coupled cavity semiconductor lasers", Appl. Phys. Lett., 1984, 44, pp. 357-377.

44 Henry, C. H. and Kazarinov, R. F. : "Stabilization of single frequency operation of coupled-cavity lasers", IEEE J.Quantum Electron., 1984, QE-20, pp. 733-744.

45 Otsuka, K. and Kobayashi, S. : "Optical bistability and non-linear resonance in a resonant-type semiconductor laser amplifier", Electron. Lett., 1983, 19, pp. 262-263.

46 Nakai, T., Ogasawara, N. and Ito, R. : "Optical bistability in a semiconductor laser amplifier", Japan. J. Appl. Phys., 1983, 22, pp. L310-L312.

47 Sharfin, W. F. and Dagenais, M. : "Room-temperature optical bistability in InGaAsP/InP amplifiers and implications for passive devices", Appl. Phys. Lett., 1985, 46, pp. 819-821.

48 Westlake, H. J., Adams, M. J. and O'Mahony, M. J. : "Measurement of optical bistability in an InGaAsP laser amplifier at 1.3 μm", Electron. Lett., 1985, 21, pp. 992-993.

49 Adams, M. J. : "Time dependent analysis of active and passive optical bistability in semiconductors", IEE Proc. Pt. J (Optoelectron.), 1985, 132, pp. 343-348.

50 Westlake, H. J., Adams, M. J. and O'Mahony, M. J. : "Assessment of switching speed of optical bistability in semiconductor laser amplifiers", Electron. Lett. 1986, 22, pp. 541-543.

51 Chen, Y. C. and Liu, J. M. : "Direct polarization switching in semiconductor lasers", Appl. Phys. Lett., 1984, 45, pp. 604-606.

52 Chen, Y. C. and Liu, J. M. : "Temperature-dependent polariz -ation behavior of semiconductor lasers", Appl. Phys. Lett., 45, pp. 731-733.

53 Uniaxial compressive stress normal to the plane of the junction lifts the valence band degeneracy, changing the relative contributions of the light and heavy hole interband transitions. See Patel, N. B., Ripper, J. E. and Brosson, P. : "Behavior of threshold current and polarization of stimulated emission of GaAs injection lasers under uniaxial stress", IEEE J. Quantum Electron., 1973, QE-9, pp. 339-341.

54 Chen, Y. C. and Liu, J. M. : "Polarization bistability in semiconductor lasers", Appl. Phys. Lett., 1985, 46, pp.16-18.

55 Liu, J. M. and Chen, Y. C. : "Optical flip-flop", Electron. Lett., 1985, 21, pp. 236-238.

56 Shore, K. A. : "Semiconductor laser bistable operation with an adjustable trigger", Opt. Quantum Electron., 1982, 14, pp. 321-326.

57 White, I. H., Carroll, J. E. and Plumb, R. G. : "Closely coupled twin stripe lasers", IEE Proc. Pt. I (SSED), 1982, 129, pp. 291-296.

58 White, I. H. and Carroll, J. E. : "New mechanism for bistable operation of closely coupled twin stripe lasers", Electron. Lett., 1983, 19, pp. 337-339.

59 White, I. H., Carroll, J. E. and Plumb, R. G . : "Room-temperature optically-triggered bistability in twin-stripe lasers", Electron. Lett., 1983, 19, pp. 558-560.

60 White, I. H. and Carroll, J. E. : "Optical bistability in twin-stripe lasers", IEE Proc. Pt. H, 1984, 131, pp. 309-321.

61 McInerney, J., Reekie, L. and Bradley, D. J. : "Observation of bistable optical effects in a twin GaAs/GaAlAs diode external cavity ring laser", Electron. Lett., 1984, 20, pp. 586-588.

62 McInerney, J., Reekie, L. and Bradley, D. J. : Bistability and instability in the output of a twin GaAs/GaAlAs diode external cavity ring laser", IEE Proc. Pt. J (Optoelectron.), 1985, 132, pp. 90-96.

63 Heffernan, D. M., McInerney, J., Reekie, L. and Bradley, D. J. : "Bistability by induced waveguiding in coupled semiconductor lasers", IEEE J. Quantum Electron., 1985, QE-21, pp. 1505-1512.

64 McInerney, J. and Heffernan, D. M. : "Optical bistability in strongly coupled, weakly guiding semiconductor lasers", SILA '86 (Inst. of Phys.), Cardiff, paper 22a.

65 Kaplan, A. E., "Optical bistability that is due to mutual self-action of counterpropagating beams of light", Opt. Lett., 1981, 6, pp. 360-362.

66 Bjorkholm, J. E., Smith, P. W., Tomlinson, W. J. and Kaplan, A. E. : "Optical bistability based on self-focusing", Opt. Lett., 1981, 6, pp. 345-347.

67 Bjorkholm, J. E., Smith, P. W. and Tomlinson, W. J. : "Optical bistability based on self-focusing : an approximate analysis", IEEE J. Quantum Electron., 1982, QE-18, pp. 2016-2022.

68 L. Reekie and J. McInerney, unpublished result.

69 Buus, J. : "Models of the static and dynamic behavior of stripe geometry lasers", IEEE J. Quantum Electron., 1983, QE-19, pp. 953-960.

70 Kirkby, P. A., Goodwin, A. R., Thompson, G. H. B. and Selway, P. R. : "Observations of self-focusing in stripe geometry semiconductor lasers and the development of a comprehensive model of their operation", IEEE J. Quantum Electron., 1977, QE-13, pp. 705-719.

71 Sommers, H. S., Jr., : "A survey of optical nonlinearities : theory and observation in (AlGa)As injection lasers", IEE Proc. Pt. I (SSED), 1982, 12, pp. 262-266.

72 Hakki, B. W. : "GaAs double heterostructure lasing along the junction plane", J. Appl. Phys., 1975, 46, pp. 292-303.

73 Marburger, J. H. and Felber, F. S. : "Theory of a lossless nonlinear Fabry-Perot interferometer", Phys. Rev. A, 1978, 17, pp. 335-347.

74 Bischofberger, T. and Shen, Y. R. : "Theoretical and experimental study of the dynamic behavior of a nonlinear Fabry-Perot interferrometer", Phys. Rev. A, 1979, 19, pp. 1169-1176.

75 Goldstone, J. A. and Garmire, E. M. : "On the dynamic response of nonlinear Fabry-Perot interferometers", IEEE J. Quantum Electron., 1981, QE-17, pp. 366-374.

76 Lee, Y. H., Warren, M., Olbright, G. R., Gibbs, H. M., Peyghambarian, N., Venkatesan, T., Smith, J. S. and Yariv, A : "Streak-camera observation of 200-ps recovery of an optical gate in a windowless GaAs etalon array", Appl. Phys. Lett., 1986, 48, pp. 754-756.

77 Silberberg, Y., Smith, P. W., Miller, D. A. B., Tell, B., Gossard, A. C. and Wiegmann, W. : "Fast multiple quantum well absorber for mode locking of semiconductor lasers", in "Picosecond electronics and optoelectronics" (G. A. Mourou, D. M. Bloom and C. H. Lee, eds.), Springer-Verlag, Berlin, 1985, pp. 159-162.

78 Shore, K. A. and Rozzi, T. E. : "Transverse mode oscillations at GHz frequencies in stripe-geometry lasers", Opt. Quantum Electron., 1982, 14, pp. 465-466.

FIGURE CAPTIONS

FIGURE 1

Representations of the characteristic curve of a bistable device : (a) experimental, and (b) theoretical.

FIGURE 2

Semiconductor laser systems which have demonstrated absorptive optical bistability :

(a) segmented contact laser;

(b) twin diode external cavity laser.

FIGURE 3

The cleaved-coupled-cavity (C^3) laser, which has exhibited bistability due to gain saturation above threshold .

FIGURE 4

Dispersive bistable systems demonstrated to date :

(a) diode in frequency selective external cavity;

(b) cleaved-coupled cavity;

(c) Fabry-Perot laser amplifier.

FIGURE 5

Laser devices exhibiting waveguiding bistability :

(a) closely coupled twin stripe laser (after White et al. [60]);

(b) self-focused coupled cavity laser (SCCL).

FIGURE 6

Experimental implementation of the SCCL : two 20 μm oxide stripe GaAs/GaAlAs laser diodes LD1, LD2 are AR coated and coupled by lenses L1-L4 via the external ring cavity formed by the mirrors M1-M4. [61].

FIGURE 7

Experimental light-current characteristic of the SCCL with one fixed current, displaying a hysteresis loop above threshold.

FIGURE 8

Theoretical light-current characteristic of the SCCL with fixed I_2 = 160 mA, displaying a slight bowing nonlinearity but no bistability.

FIGURE 9

Theoretical light-current characteristic of the SCCL with fixed I_2 = 210 mA, exhibiting bistability.

FIGURE 10

Schematic diagram of passive bistable system using a self-focusing nonlinearity (after Bjorkholm et al. [67]. L is a linear focusing lens, A an aperture and M the feedback mirror.

FIGURE 11

Simplified picture of spatial hole burning in wide stripe lasers :

(a) injected current density distribution;

(b) subtractive recombination current density;

(c) resulting carrier density distribution near threshold;

(d) assumed refractive index distribution resulting in self-focusing.

VALUES OF PARAMETERS USED IN CALCULATION OF LIGHT-CURRENT CHARACTERISTICS

laser wavelength	λ	870 nm
laser diode length	L	500 μm
laser diode stripe width	W	17 μm
active region thickness	d	0.2 μm
active region refractive index	n_{act}	3.60
passive layer refractive index	n_{pass}	3.40
effective refractive index	n	3.54
group refractive index	n_g	4.30
spontaneous emission fraction	β	$1\cdot10^{-3}$
linear index-carrier coefficient	$\Delta' = -dn_{act}/dN$	$5\cdot10^{-27}$ m^3
diode discrete loss	α_{act}	10 cm^{-1}
passive layer loss	α_{pass}	20 cm^{-1}
gain parameters †	a	$3\cdot10^{-20}$ m^2
	b	400 cm^{-1}
loss parameters †	a'	$1\cdot10^{-21}$ m^2
	b'	15 cm^{-1}
effective reflectivity	R	0.40
spontaneous carrier lifetime	τ_{sp}	2.5 ns

† : values of gain and loss parameters obtained from Buus(1983).

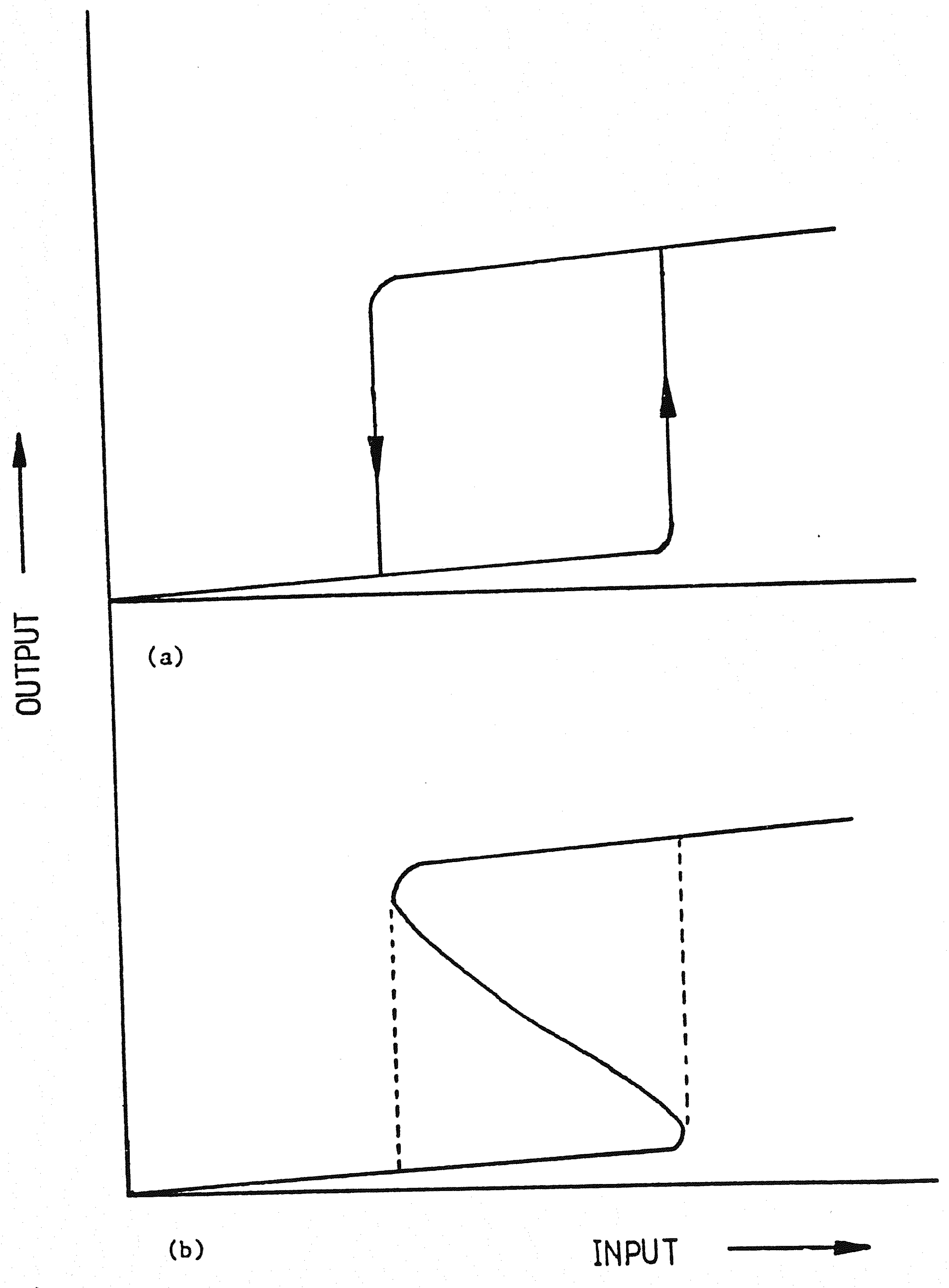
OUTPUT
(a)
(b)
INPUT

ABSORPTIVE BISTABILITY IN SEMICONDUCTOR LASERS

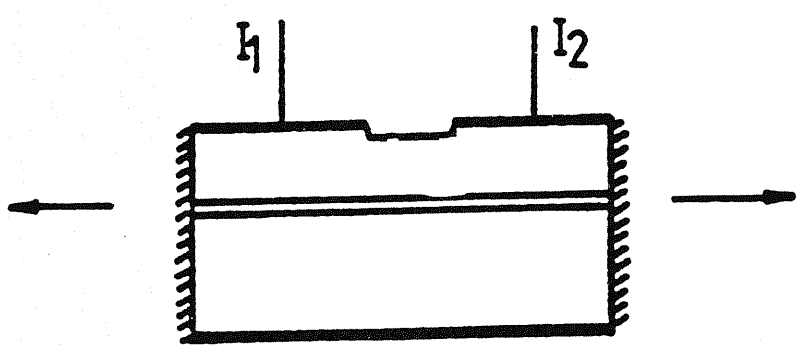

(a) segmented contact laser

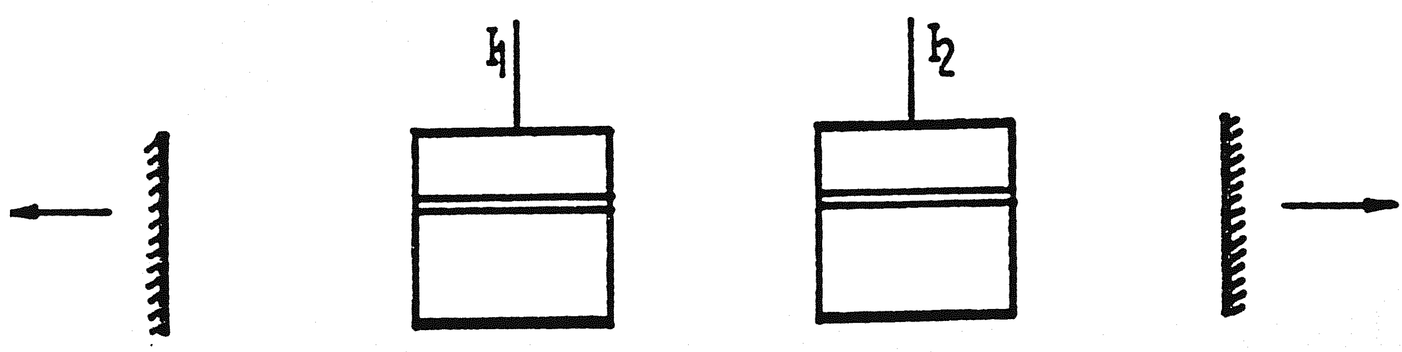

(b) twin diode external cavity laser

BISTABILITY BY GAIN SATURATION

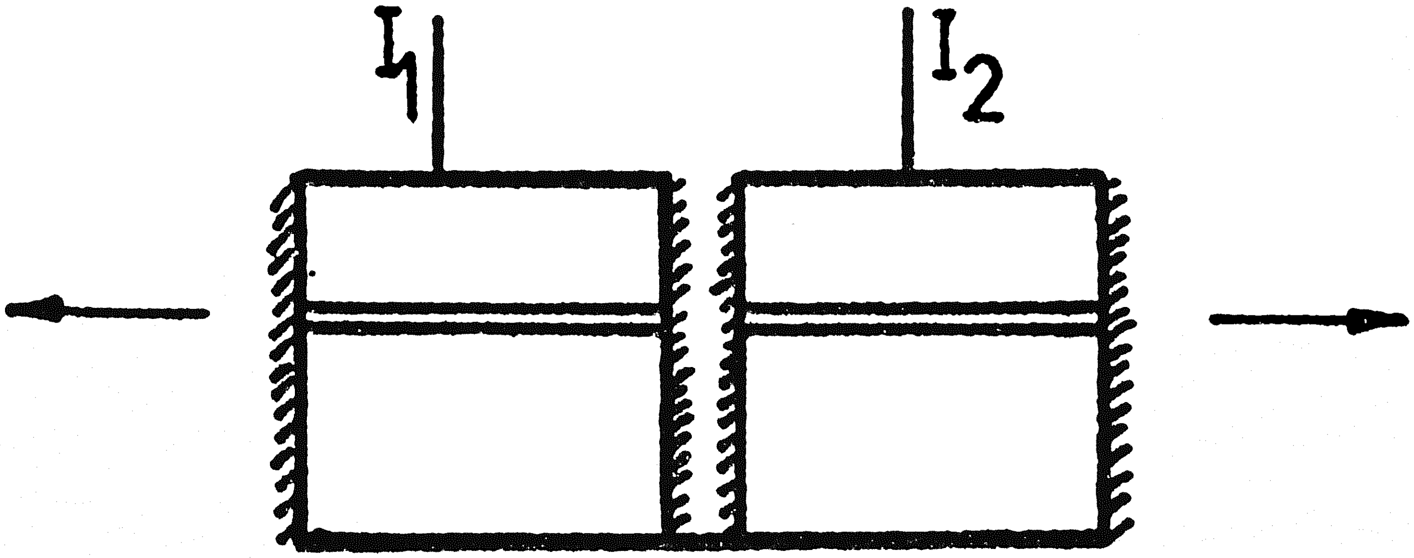

C^3 laser

DISPERSIVE BISTABILITY IN SEMICONDUCTOR LASERS

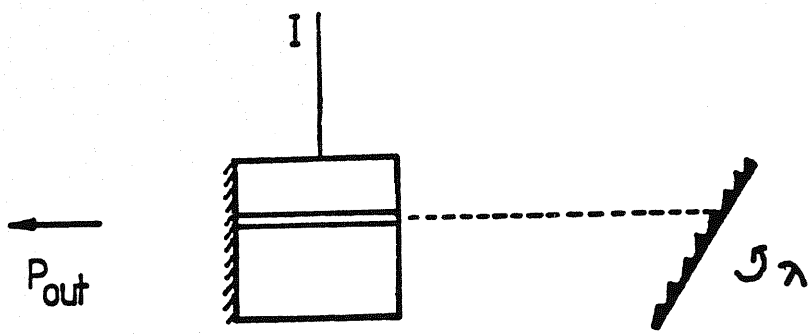

(a) dispersive external cavity laser

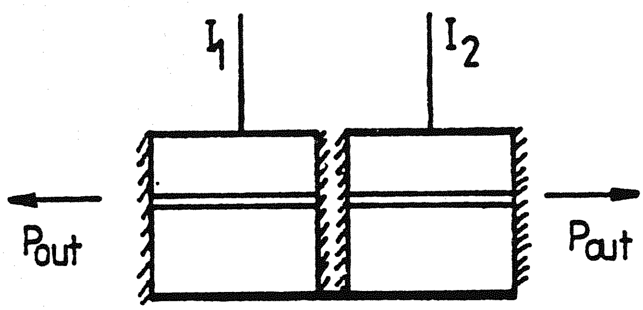

(b) C^3 laser

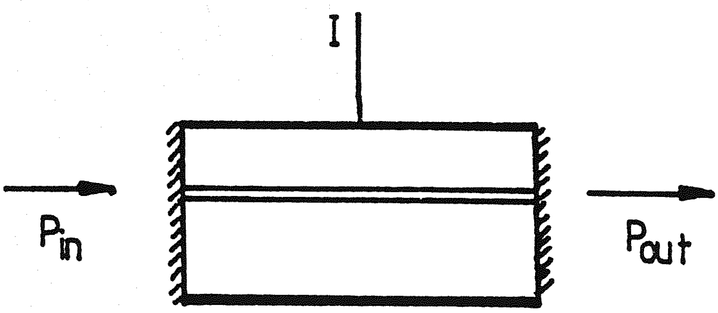

(c) FP laser amplifier

WAVEGUIDING BISTABILITY IN SEMICONDUCTOR LASERS

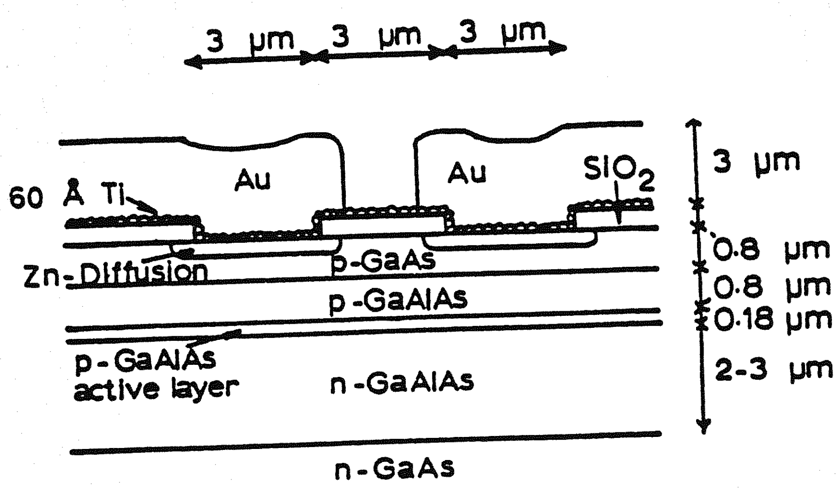

(a) twin stripe laser

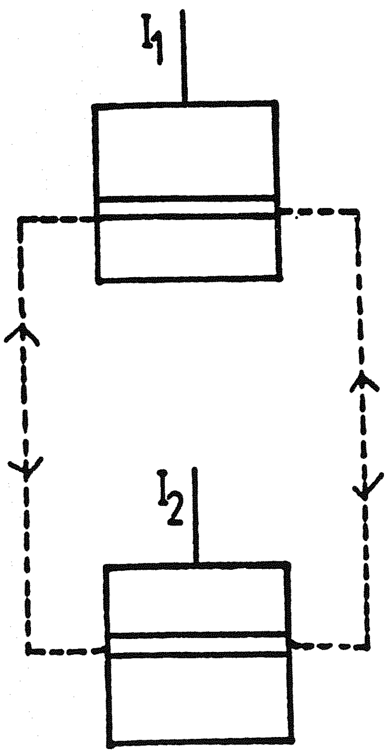

(b) self-focused ring laser

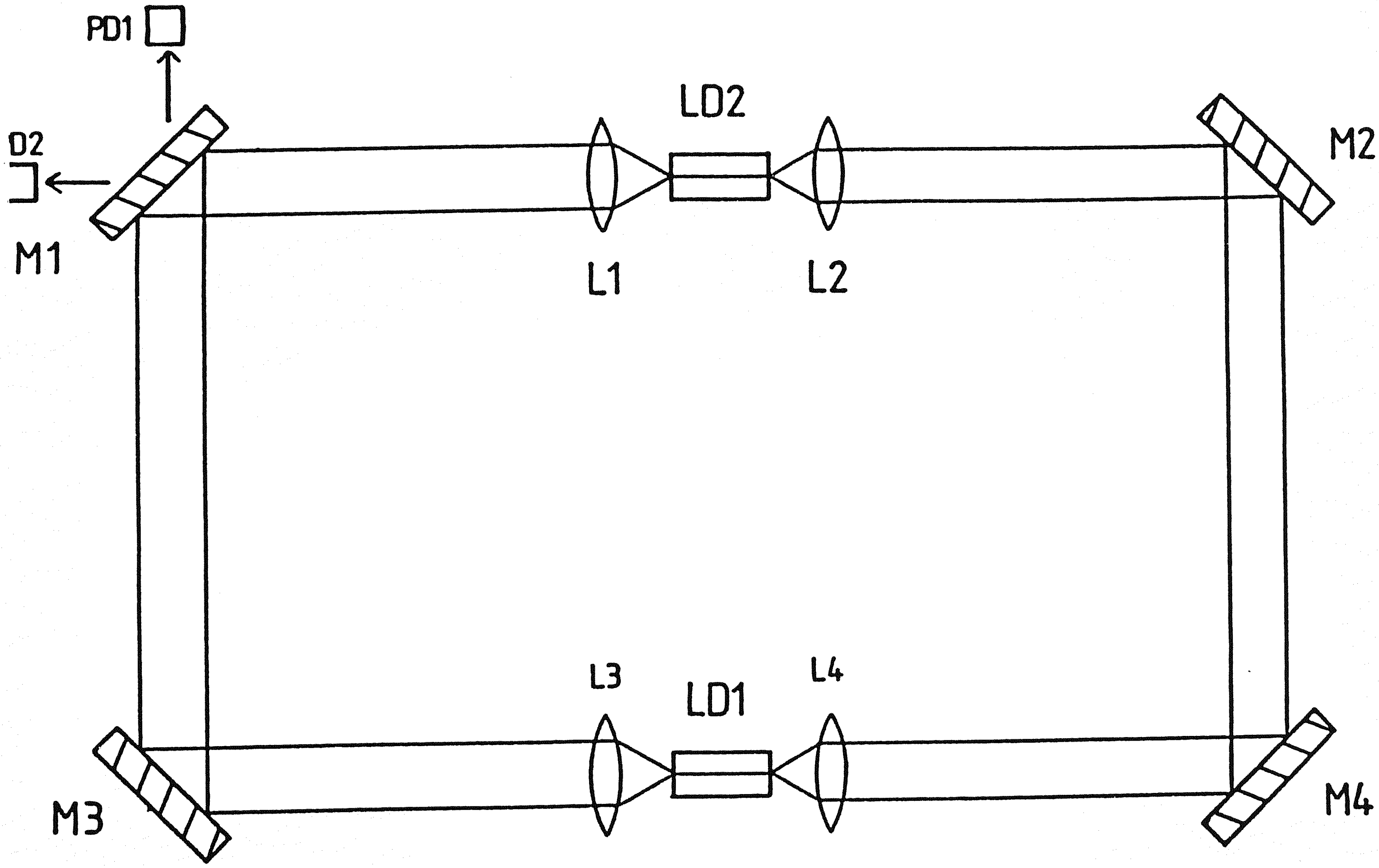

THE SELF-FOCUSED, COUPLED CAVITY LASER (S.C.C.L.)

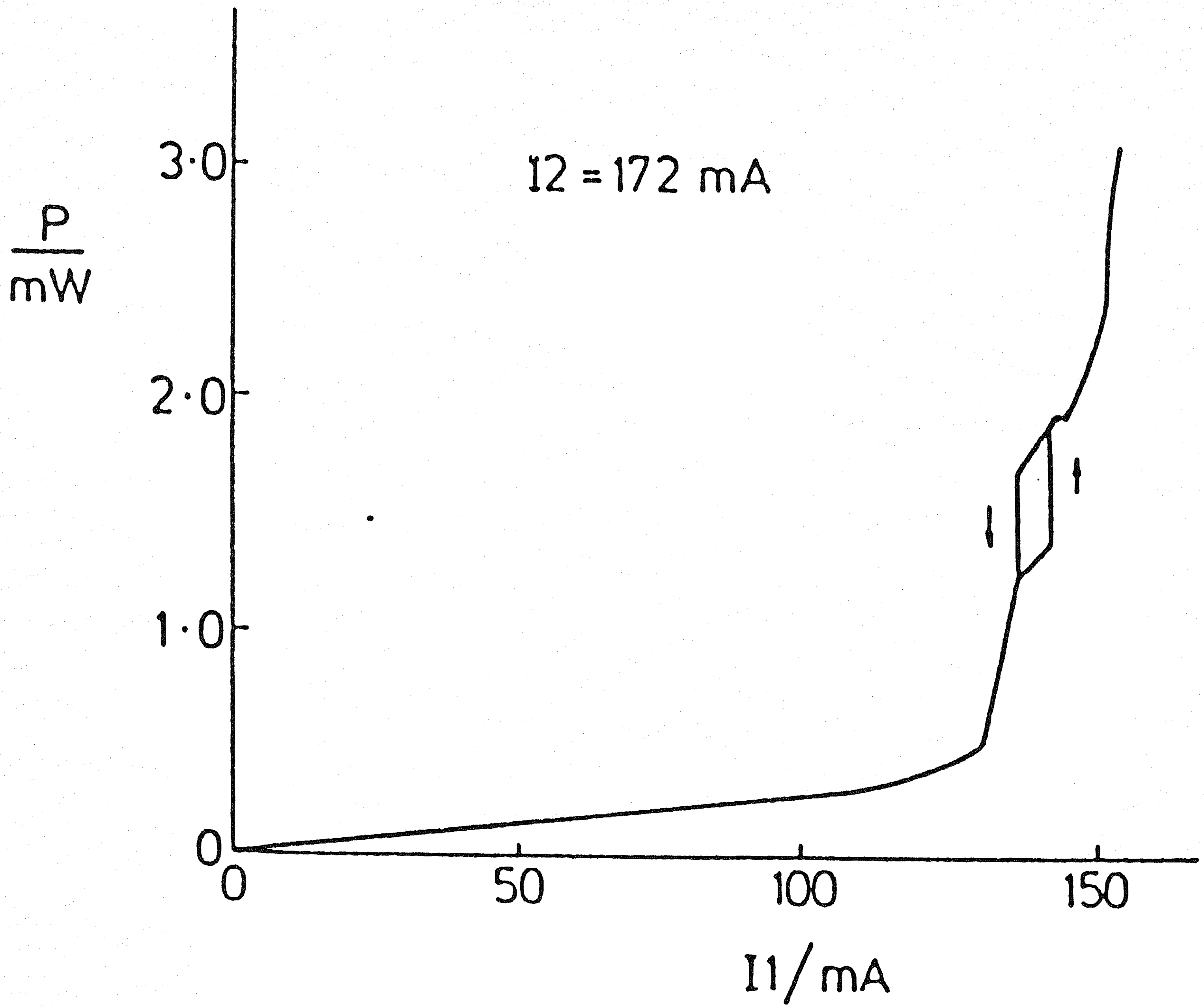

I2 = 172 mA
P / mW
3·0
2·0
1·0
0
0
50
100
150
I1/mA

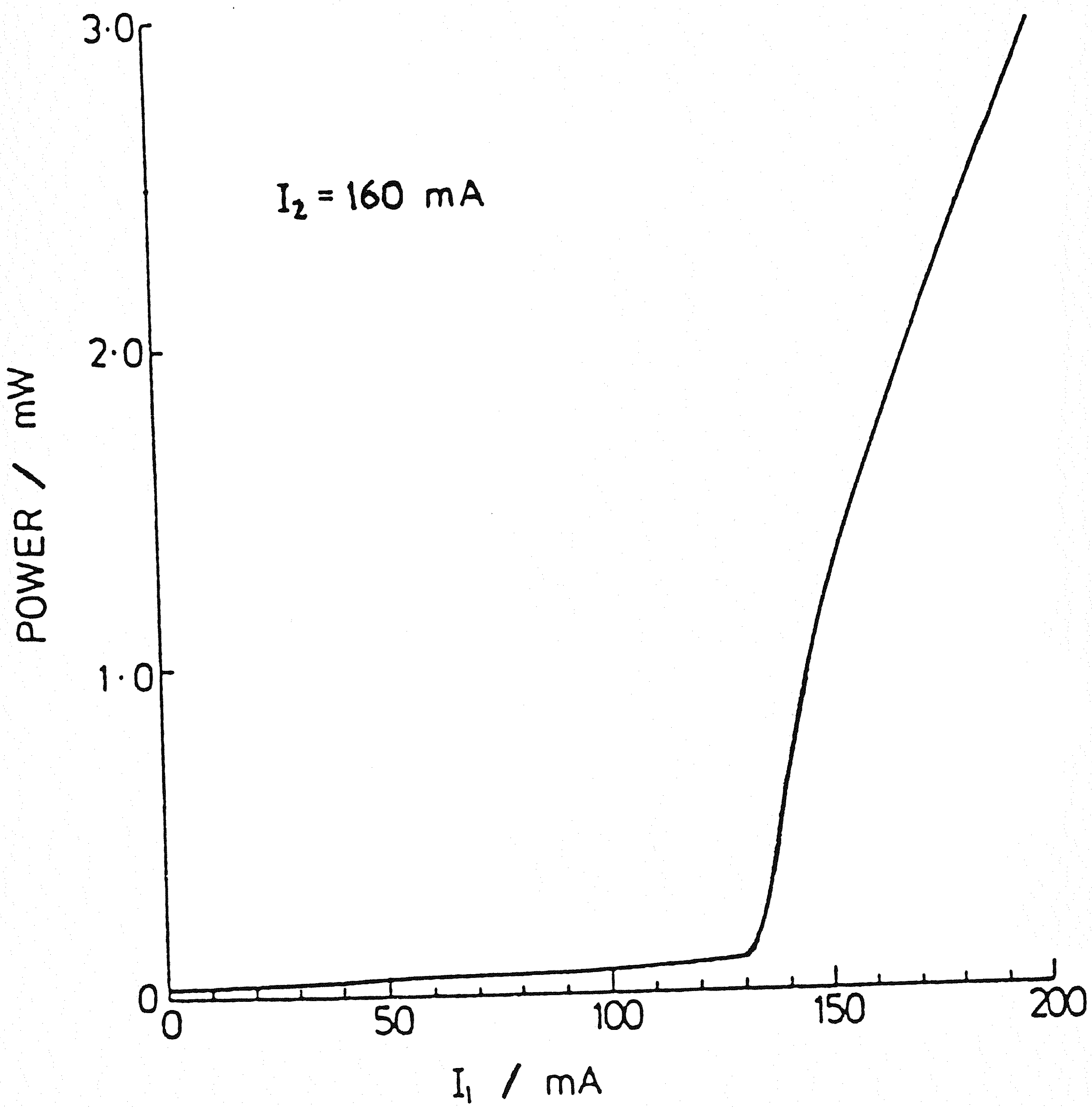

POWER / mW
3·0
2·0
1·0
0
I₂ = 160 mA
0
50
100
150
200
I₁ / mA

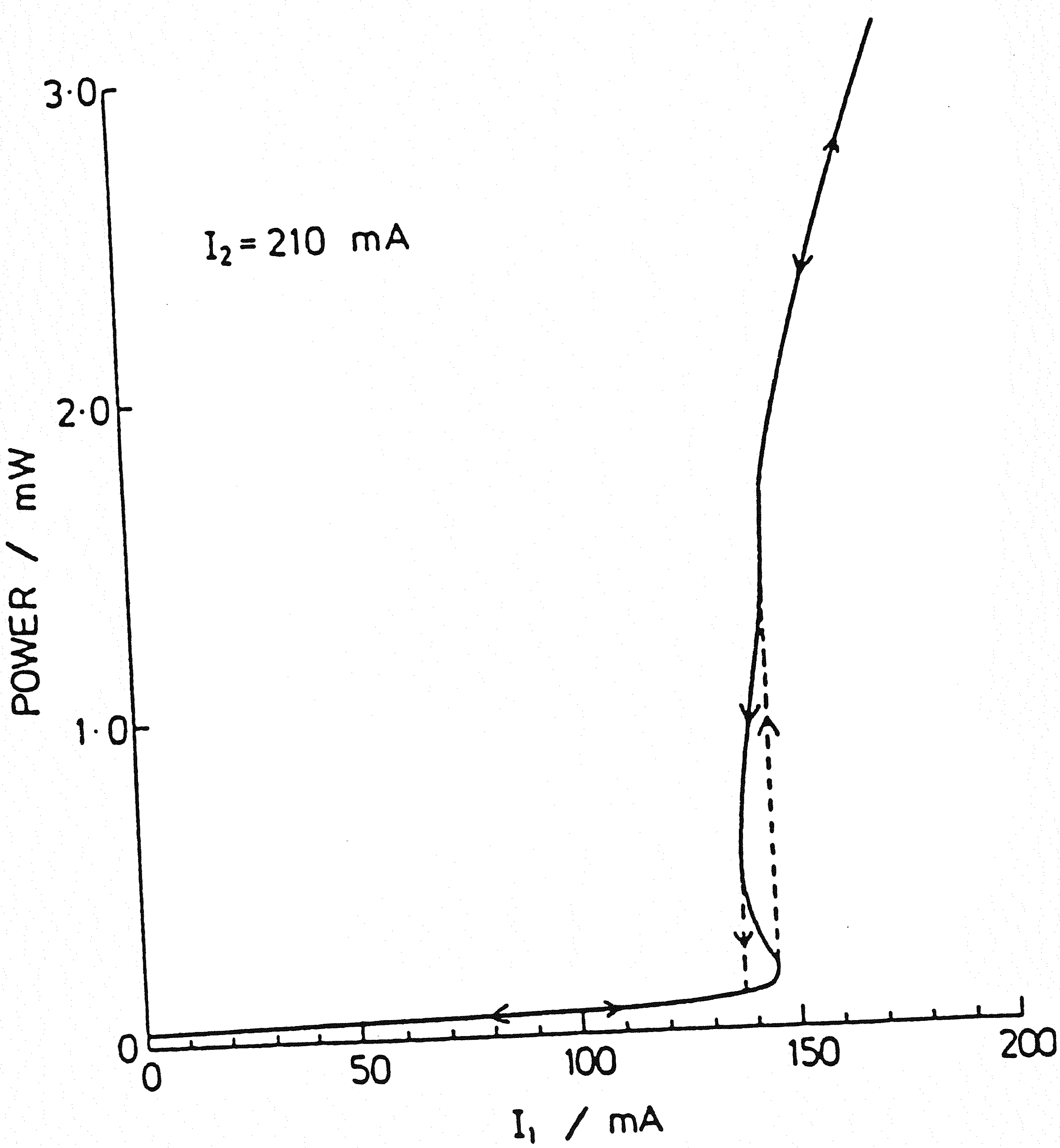

3·0
2·0
1·0
0
POWER / mW
I₂ = 210 mA
0
50
100
150
200
I₁ / mA

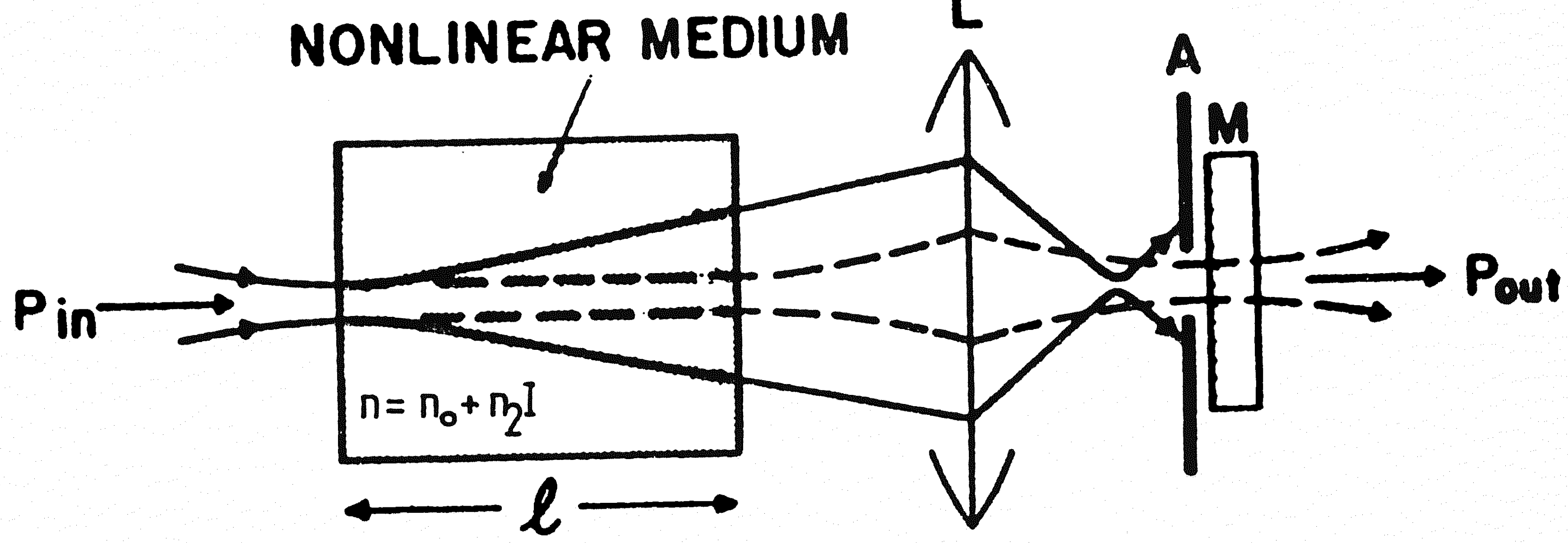
NONLINEAR MEDIUM
L
A
M
P in
P out
n= n_o + n_2 I
ℓ

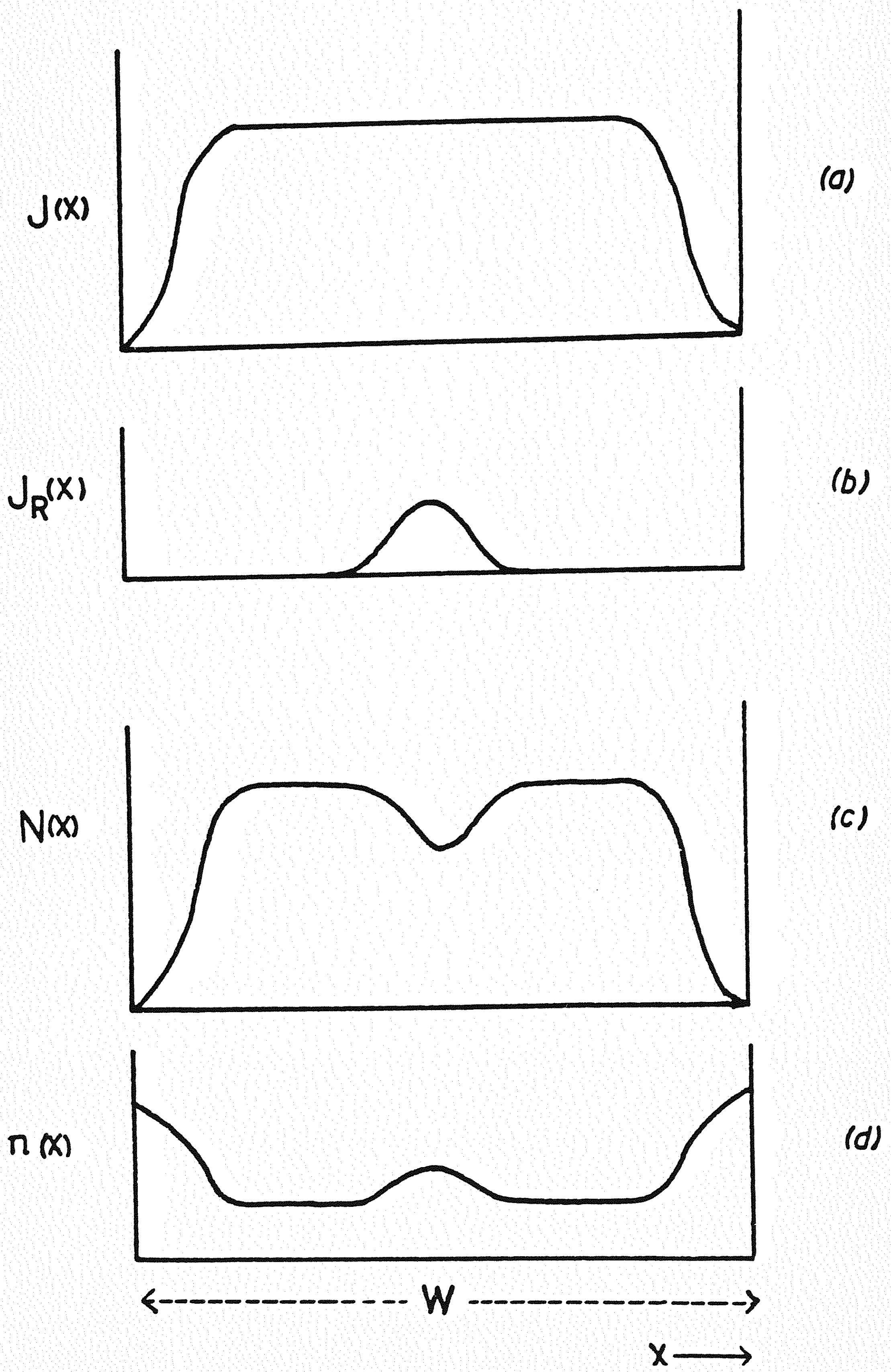

J(X)
(a)
J_R(X)
(b)
N(X)
(c)
n (X)
(d)
W
X